

Economical deployment of quarry minerals for land-based enhanced weathering in Northern California

Hanna M. Breunig^{1*}, Patricia Fox², Jeremy Domen^{3,4}, Ram Kumar^{3,5}, Ricardo Jorge Eloy Alves², Kateryna Zhalnina⁶, Anne Voigtländer³, Hang Deng⁷, Bhavna Arora³, Peter Nico³

1. Energy Analysis and Environmental Impacts Division, Energy Technology Area, Lawrence Berkeley National Laboratory, Berkeley, California, U.S.A., 94720
2. Climate & Ecosystem Sciences Division, Earth and Environmental Sciences Area, Lawrence Berkeley National Laboratory, Berkeley, California, U.S.A., 94720
3. Energy Geosciences Division, Earth and Environmental Sciences Area, Lawrence Berkeley National Laboratory, Berkeley, California, U.S.A., 94720
4. Physicians, Scientists, and Engineers for Healthy Energy, Oakland, California, U.S.A., 94612
5. Energy & Environment Science & Technology, Idaho National Laboratory, Idaho Falls, Idaho, U.S.A., 83415
6. Environmental Genomics and Systems Biology Division, Biosciences Area, Lawrence Berkeley National Laboratory, Berkeley, California, U.S.A., 94720
7. Department of Energy and Resources Engineering, College of Engineering, Peking University, Beijing, China, 100871

*Corresponding Author

ABSTRACT

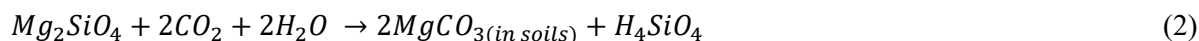
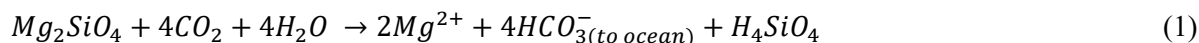
Enhanced weathering (EW) is a CO₂ removal (CDR) and sequestration strategy that accelerates the natural reactions of minerals that can store carbon from the atmosphere and biotic reactions. One method of EW is to apply finely ground silicate rocks to agricultural lands. EW has been demonstrated in laboratory and field tests, but great uncertainty remains regarding the life-cycle of using locally available rocks on candidate soils. We evaluate the life-cycle impacts, job creation, and cost of scenarios where fines and rocks mined from quarries in Oregon and Northern California are transported by truck and tilled into agricultural soils. Candidate quarry dust samples were classified as dacite, andesite, and olivine-bearing rocks, with EW potentials ranging from 125-760 kg CO₂/metric tonne rock. We determined the olivine-bearing rock from Southern Oregon could achieve a levelized cost of CDR under the DOE Earthshot target of \$100/t CO₂, as long as application rates are 25 t/ha or more. Even andesite and dacite materials reach lower costs than commercial direct air capture technologies, with reduction in fines purchase and transport costs critical for achieving the Earthshot target. The results suggest that low-cost EW can be achieved using natural quarry materials, with average removal up to 2.2 t CO₂e per hectare per year.

1. INTRODUCTION

Silicate rocks rich in base cations such as magnesium and calcium can react with carbonic acid and sequester carbon dioxide (CO₂) as solid carbonates (the process of carbonation) or dissolved bicarbonate that eventually is exported to oceans to contribute to ocean alkalinity (the process of enhanced weathering: EW).^{1,2} These processes occur naturally, but can in theory be replicated using engineered pathways to remove large quantities of carbon from the atmosphere over time scales relevant to the climate crisis.

Potential global carbon removal by way of land-based EW (i.e. surficial EW) has been estimated based on the availability of silicate rocks with low silica-content, such as ultramafic and mafic rocks.^{3,4} In land-based EW, rocks are ground to fine particle size and spread on soils or beaches to sequester CO₂ from the atmosphere *ex situ*. Basalts are frequently used in EW studies, and are abundant mafic rock with high concentrations of minerals that weather relatively quickly, including Ca-Mg Pyroxenes, Ca-Plagioclase, and sometimes olivine. Estimates of lower-bound cost for land-based EW range from \$20-200/t CO₂ removal,^{2,5-7} suggesting both the potential to achieve the United States Department of Energy “Earthshot” levelized cost target of \$100/t CO₂ removal, as well as significant sensitivities to material composition and modeling assumptions. A levelized cost is a performance metric that accounts for capital and operating expenditures over a project lifespan. These recent studies have brought attention to EW as a decarbonization pathway, but raise questions regarding both the fundamental geochemical processes driving weathering rates and the economic potential of using local quarry rocks.

Geochemical studies use specific chemical compositions to represent rock samples, and therefore lean towards endmember minerals. One endmember of olivine is forsterite (Fo: Mg₂SiO₄) which is not easily found in pure form, but represents a theoretical optimal model mineral. For example, pot studies aimed at understanding the effects of EW on crop growth and nutrient uptake use a Fo dominated olivine.⁸ Wollastonite (CaSiO₃) is another mineral used to represent silicate weathering.⁹ Weathering and carbonation of Fo can be calculated using **Equation (1) and (2)**; not shown is the reaction of CO₂ and water to carbonic acid.



In reality, candidate rocks contain a range of minerals, which leads to complex and non-idealized reactions, necessitating mesocosm studies and field trials using locally available quarry materials to verify performance. Some rock types typically ignored in EW literature are now being discussed and used in California EW pilots,¹⁰ including aggregate fines and mine tailings.¹¹ In Northern California, EW tests are being performed with a material labeled “meta-basalt” from Later Jurassic volcanic units from an aggregate quarry in Ione, California, which we classify herein as dacite.¹² Due to its higher silica concentration, dacite does not continue olivine series minerals but still contains pyroxenes and plagioclase, although in lower amounts than basalts, and therefore has various degrees of EW potential. Recent advancements in the measurement and simulation of weathering kinetics, and associated processes, including experiments conducted by some of the authors on dacite fines from the same aggregate provider in Northern California, have shed light on factors affecting CO₂ removal.^{3,13} Example

factors include proper soil selection, and adequate tilling into soils to ensure particles are exposed to the soil and to potentially introduce more air and thus atmospheric CO₂.¹³ However, understanding the environmental impacts and cost of deploying a local rock on appropriate nearby agriculture land with tilling requires an understanding of the full life-cycle of EW projects at meaningful and realistic deployment scales. Life Cycle Assessment (LCA) of land-based EW exist, including a study on the use of materials from new basalt quarries in Brazil.¹⁴ That study provided valuable insights on key sources of emissions, including identification of cutoff distances for diesel transportation of rock to field. Other environmental evaluations consider idealized rocks,^{15,16} or simply apply cost and emissions values from previous literature without bottom-up modeling. No framework existed for explicit bottom-up models of life-cycle processes or the coupling with an economic analysis, particularly in a northern-hemisphere economy, until Zhang and colleagues.^{14,17} In that study, representative capture potentials reflecting possible rock fines and sands from copper mines are used (0.2-1.1 t CO₂/t rock), with supply chains modeled as barge and truck transport to agriculture lands in the Midwest U.S. Life cycle capture potential of 225-1020 kg CO₂e/t material was estimated at costs ranging from \$45-472/net t CO₂e removal. With few exceptions,^{17,18} cost estimates are rarely conducted alongside LCA, which limits the ability to adjust levelized cost \$/t CO₂ removal to \$/net t CO₂e removal.

This work builds on previous LCA¹⁴ and economic analysis⁷ by developing more detailed bottom-up models of key life-cycle processes for a large EW deployment project in Northern California. We leverage information from an existing 40 hectare pilot project in the area operated by the University of California Office of the President Working Lands Innovation Center (WLIC),¹² and assume a deployment at the scale of 100,000 tonnes of olivine-bearing rock, dacite or andesite fines, or “produced-for-purpose” olivine-bearing quarry rock on 900 hectares of cropland within 80, 447, or 1037 km in 30 years. These distances are trucking route distances going from regional quarries where samples were collected to the WLIC agriculture area. Application is capped at 111 t per hectare (45 t/acre), while the frequency of application is limited based on rock dissolution rate and land management practices. As such, necessary annual production of rock material varies across scenarios included in this study, but is expected to be less than ~4% output of a medium-size aggregate quarry with an annual output of 450,000 tonnes. We approach EW from the perspective of an EW company that partners with an existing aggregate quarry, where the EW company is responsible for the purchase, staffing and operation of necessary comminution equipment that is unlikely to already be at aggregate mines for the produced-for-purpose materials, front loaders, highway suitable truck fleets, and tractors. If the EW company does not purchase the equipment, it is reasonable to expect a specialized starting material to have a higher upfront cost. We discuss the use of mine tailings that could potentially be freely available for use in section 3.6.

The novelty of this work lies in the coupling of the LCA with the economic analysis, but more importantly the use of current local rocks from aggregate quarries including those that have been overlooked in literature such as andesite and dacite, and the bottom-up modeling of key processes including the effect of particle size and weathering rates on life-cycle processes that are time dependent and allow for estimates of labor. While job creation ultimately varies throughout the lifespan of a project and by business, there are methods to bound potential job creation and quality. Herein, we use an equivalent equipment module approach, where job creation, salary and type are determined based on location, equipment type and shift requirements. These contributions provide much needed data on the potential for scaling enhanced weathering.

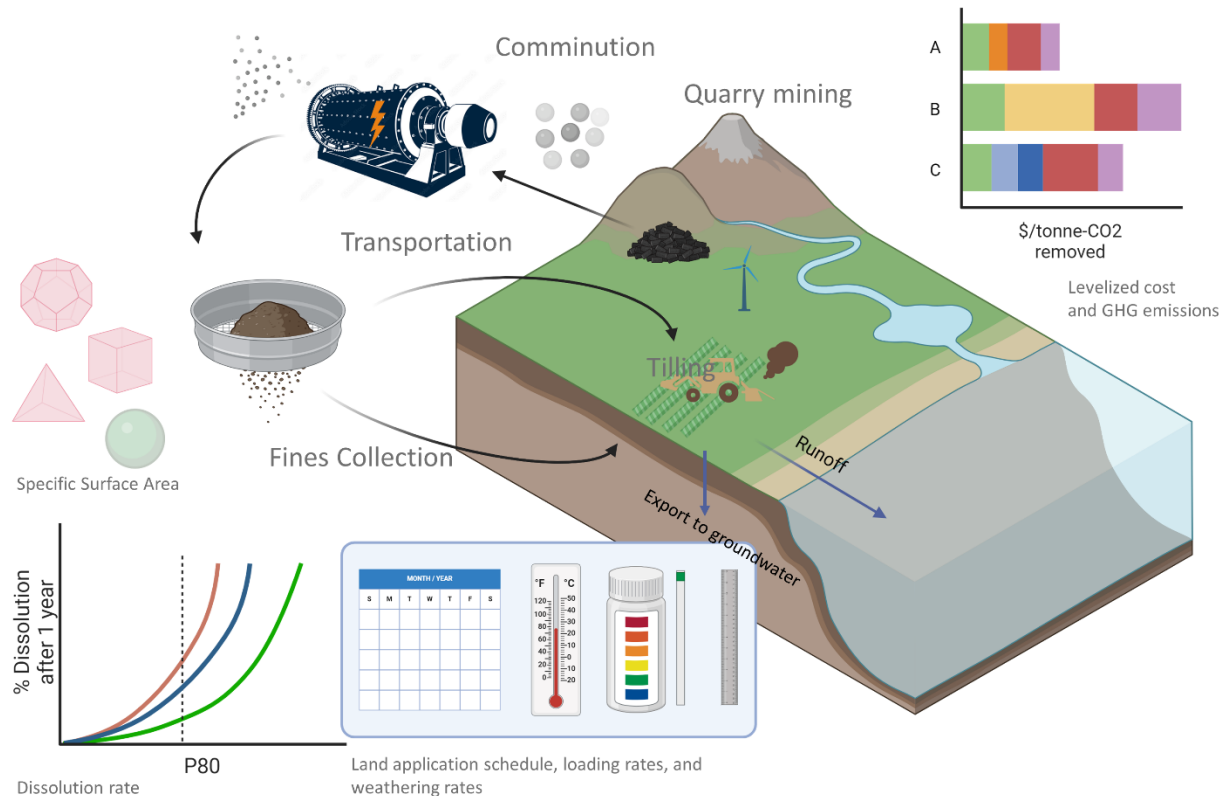


Figure 1. Schematic of the analysis presented in this study. The analysis includes the selection of rock materials and estimation of theoretical mineral carbon removal potential, the impact of target grain size, the impact of specific surface area and particle shape on dissolution rates, and an evaluation of variables affecting life cycle cost and greenhouse gas emissions. Variables include the loss of ultrafine particles prior to land application, energy sources, transportation requirements, field application rate affected by tractor type, farmer preferences and variables affecting dissolution such as rainfall, temperature and pH.

2. MATERIALS AND METHODS

The LCA follows the ISO 14040 and 14044 standard structure, which includes goal and scope definition, Life-Cycle Inventory (LCI) development, life-cycle impact assessment (LCIA), and results interpretation, as detailed in the following sections. Bottom-up modeling was used to represent key sub-processes in the LCI, while background data for quarry blasting was generated using both the United States Life Cycle Inventory (USLCI) and ecoinvent3.2 databases.¹⁹ Calculations were performed in OpenLCA2.0 to convert CO₂, CH₄, and N₂O into CO_{2eq} based on global warming potentials (GWP), and to convert other emissions including nitrogen oxides (NO_x), SO₂, and particulate matter (PM_{2.5}) into impacts of importance (see ESI for details). We used the GWP results of the LCA in our cost analysis to obtain levelized cost of carbon removal (\$/net t CO_{2e} removed).

2.1 System Boundary.

The system boundary of the LCA and cost analysis includes flows of capital, labor, and operation materials and energy for the following processes for produced-for-purpose olivine-bearing rock: material extraction at the quarry, material transport within the quarry to the grinding facility, material grinding with ball milling, material transportation to fields on public roads, and material loading and spreading on fields by diesel tractor and till. The flow of processes at the mine follow the suggested operation pathway proposed in Renforth 2012 (see Figure 5²⁰ for flow path of materials during comminution). For existing by-products of quarries such as fines, we only account for material collection, transport and application. The functional units are one tonne of rock material applied, and one tonne of net-CO_{2eq} removed.

Total allowable application rates vary in literature, but we assumed 111 t material/ha over the project lifetime, and explore the impact of scenarios where only 1 mm thickness of material application is allowed per pass. Single applications for EW experiments have been relatively low (e.g. 3 t/ha)⁹ while analysis have evaluated application rates from 2-494 t/ha, with base cases around 40-111 t/ha.⁷ A single pass of 111 tonnes at a base case bulk density of 1800 kg/m³ would result in a thickness of 6.19 mm. As such, the project area could be treated in ~6 passes in 6 years and 3 months if the annual dissolution rate is 100%. For a project deploying 100,000 tonnes of rock material locally on 900 hectares of treatable area, the maximum rock material required annually would be 16,155 tonnes, which is ~3-4% of the output of a medium sized quarry. As such, we do not consider the quarry to be dedicated to EW and do not attribute any land use change in our analysis. In all cases, we assume a constant influx of fresh rock (and thus constant CDR removal through weathering reactions) is applied as soon as the material is dissolved, assuming each tractor pass applies 1 mm of material.

We select a study region around Davis, California, where land-based EW trials are currently ongoing. Davis, California receives an average of 50 cm/yr of rainfall, and is in a region with plentiful silicate rocks which bear high percentages of olivine deposits.^{12,21} We acquired a particle size analysis, mineral analysis, and total elemental analysis for regional olivine-bearing rock samples from an unknown quarry in Oregon, and local rock samples from Specialty Granules, Inc. in Ione, California, provided by the WLIC. We classified samples using the Total Alkali Silica method to assist us in down selecting representative rock compositions (see ESI for details). In regards to grinding, we assume olivine-bearing rocks are not available as fines in California and thus must be processed down to a P80 of 0.179 mm,

which is the P80 of the local rock samples. P80 is the mesh size at which 80% of materials pass through. Rocks applied on land are modeled as having uniform size, however in reality a size distribution is generated and smaller particles which will have more rapid dissolution rates.

Region-specific ranges were identified for the following key parameters: (1) weathering performance derived from CDR potential (E_{pot} : g CO₂ /g material), P80 (mm), Specific Surface Area (SSA: g/m²), and dissolution rates based on SSA and location conditions; (2) supply chain conditions derived from fuel price, electricity price, bulk density, land application load rate, land area treated, transportation distance, and equipment capacity factors; (3) sources of Scope 2 and 3 emissions derived from fuel consumption and electricity source (**Table S2**). We evaluated the impact of operational hours on overall job creation, emissions and costs, as it is possible EW companies may operate seasonally or intermittently to align with low cost, renewable electricity, or the availability of equipment.

2.2 Enhanced Weathering Model.

The EW or carbon removal potential (E_{pot}) can be approximated for rocks with more complex compositions, such as the rocks evaluated in this study (see section 3.1 for mineral classifications) based on the major element concentrations expressed as oxides using **Equation 3**.^{22,23} This approach does not account for reaction rates and simply estimates the contribution of each oxide to the divalent cations leading to enhanced weathering and the formation of carbonates.

$$E_{\text{pot}} = \frac{M_{\text{CO}_2}}{100} * \left(\alpha \frac{\text{CaO}}{M_{\text{CaO}}} + \beta \frac{\text{MgO}}{M_{\text{MgO}}} + \varepsilon \frac{\text{Na}_2\text{O}}{M_{\text{Na}_2\text{O}}} + \theta \frac{\text{K}_2\text{O}}{M_{\text{K}_2\text{O}}} + \rho \frac{\text{MnO}}{M_{\text{MnO}}} + \gamma \frac{\text{SO}_3}{M_{\text{SO}_3}} + \delta \frac{\text{P}_2\text{O}_5}{M_{\text{P}_2\text{O}_5}} \right) * 10^3 * \eta \quad (3)$$

where respective elemental concentrations of oxides (wt-%) are divided by molecular mass (M), and multiplied by coefficients derived from Renforth 2019 for a pH of 7 (**Table S1**; note that γ and δ are negative to account for phosphorus and sulfate minerals that decrease CDR). The molar ratio of CO₂ to cation transported to the ocean and sequestered (η) is assumed to be 1 when only carbonation occurs and 2 when only EW occurs. Values between 1.4 and 1.7 are used for seawater, with 1.5 being the value used in this study to account for buffering of current seawater systems.²² Uncertainties exist regarding the fate of weathering products and the transport capacities of local hydrological systems such as surface waters. Lefebvre and colleagues use a simplified equation with only CaO and MgO, and estimated carbonation and EW potential of local basalt samples in Brazil to be 0.125 and 0.225 g CO₂ per g basalt, respectively. Other estimates use a value of 1.7 for η for basalts and derive 0.3 g CO₂ per g basalt.¹⁴ Bullock and colleagues use **Equation 3** to estimate a E_{pot} of 0.938 g CO₂ per g forsterite, data originally from Le Maitre, 1982 which we use to represent forsterite.^{23,24}

We adopt the method proposed by Strefler and colleagues⁷ to estimate the percentage of mineral dissolved over the course of one year and to ensure adequate rainfall to facilitate reactions (**Equation 4**). We selected a WR representative of forsterite at pH 7 and 25°C (10^{-9.86} mol/m²-s) and hold SSA constant over time. There are limitations to this approach, as the relationship between WR, intrinsic particle characteristics and field conditions such as crop selection, soil type, application approach, and climate are poorly understood and difficult to derive from previous field and experimental trials.²⁵ Furthermore, any

potential change in SSA over time is ignored. Uncertainties related to WR are discussed in detail by Calabrese and colleagues.²⁶

$$d(x) = SSA(x) * WR * m * t \quad (4)$$

where $d(x)$ is dissolution rate (%) for a given grain size x (μm), $SSA(x)$ is specific surface area in units of $\text{m}^2 \text{g}^{-1}$ is estimated using **Equation 5**, WR is an SSA-based weathering rate in units of $\text{mole m}^{-2} \text{s}^{-1}$, m is the molecular mass in g mol^{-1} for the reference case and olivine-bearing rock, and t is a conversion from seconds to years. Molecular mass will vary by rock, but we use representative ranges identified for rocks studied in the context of EW (see ESI for details).

Empirical analysis based on measurements of SSA over a range of grain sizes suggest SSA rapidly increases with decreasing P80 (or grain size x ; μm),⁷ with annual resulting dissolution rates of 100% or higher only unlocked at $P80 < 0.02 \text{ mm}$ (**Equation 5**). This empirical approach developed for dunite by Strefler and colleagues suggests 33% of the ideal forsterite particle at 0.05 mm is removed within a year, while only 6.8% of our rock samples at 0.179 mm are removed. However, developing a robust correlation at small grain sizes is complicated by the various methods in which particles were generated for experiments, which may create different or poorly characterized particle shapes, porosity, and surface roughness that affect active mineral surface. Notably, the sample meta-andesite has a particle size distribution that leads to smaller particles and a significantly higher experimentally determined SSA than what is estimated empirically using **Equation 5**. We provide further discussion of the impact of shape and particle size on SSA in the ESI.

$$SSA(x) = 69.18 * (x)^{-1.24} \quad (5)$$

where $SSA(x)$ is specific surface area in units of $\text{m}^2 \text{g}^{-1}$, and x is P80 or grain size (μm).

2.3 Quarry Model.

Olivine-bearing rocks in California are collected from quarry face blasting and transported a short distance to primary, secondary, and tertiary crushers to first achieve an 80% pass size (P80) of <30 to $<5 \text{ mm}$.²⁰ Grinding via a ball mill further reduces particles to $P80 < 5$ to $<0.01 \text{ mm}$ to achieve a rock dust/flour. We model quarry blasting and loading of initial rock material using basalt production as a representative process. Transport within the quarry is modeled assuming diesel lorries. Crushers and grinders are operated on either renewable or local grid electricity. Capacity of the comminution equipment was set at 30 tonnes per hour to reflect a common industrial size identified in vendor quotes. The capacity of the comminution equipment is a critical uncertainty, as it affects plausible annual material production. As 20% of the total material stream turns into fines at the quarry, we expect fines for andesite and dacite to be readily available for purchase.²⁰ While these fines may be perfectly suitable for EW, their safe and effective collection and use for land application and ultimate weathering rates is an uncertainty in the supply chain. Additional material may be lost during transport and storage, but that is not considered herein.

Energy consumed per tonne of treated rock material was estimated for P_{80} greater than 5 mm from Hangx and Spiers,³ for P_{80} 1 mm to 5 mm from Renforth,²⁰ P_{80} 5 mm to 0.01 mm from Bonds Law for ball milling of basalt (**Equation 6**), and P_{80} 0.01 mm to 0.002 mm from stirred mills.²⁷ We note that ball mills are just one of several types of mills that can be applied to form small particles, and their energy efficiency and application for rocks at quarries requires further validation.

$$W = 10W_i \left(\frac{1}{\sqrt{P_{80}}} - \frac{1}{\sqrt{F_{80}}} \right) \quad (6)$$

where $W_i = 18.56$ kWh/t is the Bond work index for basalt representing ore hardness and ultimately energy for particle size reduction W (kWh/t), F_{80} is the starting size of rock material (5000 μm), and P_{80} is the target grain size.

Values were compared to reported comminution energies in literature, with good agreement between the Bond Law for basalt and recent work by Shi and colleagues.^{27,28}

2.4 Transportation Model.

Diesel heavy duty dry bulk trailer trucks with a payload of 14.5 tonnes and average fuel consumption of 2.76 kilometers per liter (6.5 mpg; 60% greater fuel consumption when full)²⁹ were assumed to be used to transport the rock dust from the supplier to the field and return empty. Payloads of this size fall under Class 7 and 8 trucks, and include vehicles such as dump trucks, refuse trucks, and truck tractors. Dry bulk trailers are used around the world for the transport of powders for plastic production and other industries. Roundtrip fuel consumption is therefore 3.26 liters diesel per tonne for the 80 km Ione quarry source where the truck is fully loaded and returns empty. We estimated the number of trucks necessary based on payload, a travel speed of 80 kilometers per hour (50 mph), 14 hour per day driver availability based on regulations. For the Ione quarry, 22 trucks would be required if all rock materials were delivered in year one. However, we assume materials are delivered each year a new application is performed, allowing for only 1 truck purchase for a project with 6 application years. The one-way distance to quarries in Southern and Northern Oregon was approximated as 447 km and 1037 km, respectively based on the geographic distribution of olivine-bearing materials.²¹ Maintenance, registration fees, and tire replacement were modeled based on data compiled by the American Transportation Research Institute.³⁰

2.5 Field Application.

It was assumed a front loader is used for loading and hauling, and two diesel tractors are used for dispensing rock dust on established agricultural land. A tractor for spray dispensing can treat on average 12 to 20 ha/engine-hour, while a tractor that plows or tills may treat 0.5 to 5 ha/engine-hour. We limit daily work to 12 hours. We assumed minimal plowing or leveling is required, but to avoid dust formation and to allow for some tilling, we conservatively chose an application rate of 2 hectares/engine-hour. The fuel consumed for dispensing the rock dust was modeled as 11 L/ha based on an average fuel efficiency of 86 L per engine-hour (23 L/hr). This is notably higher than fuel consumption for dispensing dry bulk fertilizer of ~2 L/ha, which we use to account for the added power requirement of tilling.³¹ Fuel consumption can increase by as much as 50% if the ground is not plowed at the start of the project. Fuel consumption will also depend on the soil type, with sands and sandy loams requiring 35 to 40% less fuel,

and clays and clay loams requiring 35 to 40% more than the default soil type which is a silt loam.³¹ These variations were captured in our sensitivity analysis.

2.6 Economic Analysis.

Life-cycle costs for the project include all installed capital and operating expenditures over the active project period, aligning with the time it takes to apply materials. The levelized cost of material application (\$/t rock applied), converted to the levelized cost of net-carbon removal (\$/net t CO₂e) (**Equation 7**), was determined based on the total rock applied over the course of the project. Capital costs are converted to \$2023 installed costs and annualized using a capital recovery factor approach recommended for energy systems (**Equation 8**).³² Key financial cost factors are provided in **Table S4**.

$$\text{Levelized cost of CDR} = \frac{\sum C_{\text{annual}} + \sum C_{O\&M} + \sum C_{\text{labor}}}{\text{net t CO}_2\text{e}} \quad (7)$$

where C_{annual} is the discounted capital cost determined in **Equation 8**, $C_{O\&M}$ are annual fixed and variable operating and maintenance costs, and C_{labor} is the annual cost of labor, divided by net carbon removal associated with annual material application.

$$C_{\text{annual}} = (\sum C) * \frac{(1-T_x * D_{pv})}{(1-T_x)} * \frac{i * (1+i)^l}{(1+i)^l - 1} \quad (8)$$

where T_x is tax rate, i is inflation rate, l is project duration, and D_{pv} is depreciation rate.

Costs associated with the quarry include the cost of the crushers and the ball mill for produced-for-purpose olivine-bearing rocks, the starting rock material, energy costs assuming diesel and local grid electricity, maintenance costs assuming 10% of capital cost, and the cost of labor. All costs and impacts of quarry operation are allocated based on the amount and frequency of material produced and delivered for land application. Equipment and energy costs vary and are included in the sensitivity analysis, with base values representative of current market prices in Oregon and California (**Table S2**).

Transportation includes the cost of fuel, the cost of the truck, truck maintenance, and labor. Labor is estimated based on an 80 kmph travel speed and the roundtrip total miles traveled to deliver all rock material to the fields (2 hours roundtrip per truckload from Lone and 11-26 hours from Oregon quarries, distances and energy costs approximated using Menford and Baker City as low and high values).²¹ Labor hours are then converted to truck hours per tonne based on the payload of the truck, which is then used to estimate the number of trucks per project. Field application includes the cost of the tractor, tractor maintenance assuming 10% of capital, and the cost of labor. Labor is estimated based on a tractor covering 5 acres per hour, the number of passes required for application, and the land area treated (2,745 hours per project, see ESI for details).

3. RESULTS AND DISCUSSION

Results of the life cycle impact and cost assessment of EW based on regional aggregate quarry fines and possible produced-for-purpose rock materials are presented below.

3.1 Mineral Classification, CDR Performance, and Dissolution Rate.

Out of the rock fines samples analyzed, the olivine-bearing sample sourced from Oregon had a CDR potential (E_{pot}) of 760 kg CO₂/t rock, matching what is expected of olivine rock, and therefore a prime target for enhanced weathering.²³ Two meta-andesite samples had CDR potentials over 150 kg CO₂/t rock, while the dacite samples fell between 120 and 128 kg CO₂/t rock (**Table 1**). Major element oxide concentrations were present in the rock samples, except for SO₃, and FeO which was reported in the form of Fe₂O₃. As summarized by Bullock et al, the presence of P and S bearing materials reduced CDR potential, and high Al and Fe also reduced CDR potential depending on pH, as they form insoluble secondary materials during the weathering process.²³ The pure forsterite we use to benchmark fines samples has an ultra-high CDR potential of 938 kg CO₂/t rock.

Particle shapes with more surface and surface roughness than spheres, and particle porosity can increase SSA (**Figures S1**).⁷ Doubling SSA for the same particle grain size would have a significant impact on dissolution, with impacts on the same order of magnitude as temperature and pH (**Figure S2**).⁷ In general our selection of SSA are low but result in predicted dissolution rates that match what we measure in mesocosm studies. Measurements of SSA for forsterite are much higher in literature than what we estimate empirically in this study (9.5 m²/g for forsterite with a P80 of 0.044 mm, compared with 0.54 m²/g at P80 of 0.05 mm). Furthermore, we experimentally measured an SSA of 2.23 m²/g for the meta-andesite sample (compared with our empirical value of 0.11 m²/g at P80 of 0.179 mm).³³ Using the upper range of SSA values for samples along with our default WR in Equation 3 generates dissolution rates that are far too high. So, even if we acknowledge using low SSA values, the resulting dissolution rates we adopt in this study align with that seen in our field work. This suggests a major lack of correlation and understanding regarding particle optimization and target dissolution, which may not be a concern on very long time scales, but will be when working with land owners to identify acceptable application rates.

Table 1. Representative rock sample analysis results. E_{pot} : weathering potential calculated in this study. TAS: total alkali silica classification method.

Sample Name	SiO ₂ (wt%)	TiO ₂ (wt%)	Al ₂ O ₃ (wt%)	FeO (Fe ₂ O ₃) (wt%)	MnO (wt%)	MgO (wt%)	CaO (wt%)	Na ₂ O (wt%)	K ₂ O (wt%)	P ₂ O ₅ (wt%)	Cr ₂ O ₃ (wt%)	BaO (wt%)	LOI (wt%)	Sum (wt%)	Na ₂ O + K ₂ O (wt%)	TAS symbol	E_{pot} (kg CO ₂ /t)
Forsterite	42.7	0.00	0.00	0.00	0.00	57.30	0.00	0.00	0.00	0.00	0.00	0.00	0.00	100.00	0	Pc	938
Olivine Rock	41.43	0.02	0.57	8.34	0.12	46.13	0.21	0.06	0.04	<0.01	0.56	<0.01	2.2	100.07	0.1	Pc	760
Meta-Andesite	61.66	0.54	15.05	6.52	0.16	3.27	5.19	3.36	1.28	0.15	0.01	0.06	2.6	99.91	4.64	O2	160
Meta-Dacite	65.51	0.52	15.61	4.85	0.12	1.84	3.9	3.56	1.54	0.17	0.01	0.06	2.2	99.91	5.1	O3	125
Quartz rock	99.65	<0.01	0.04	0.2	<0.01	<0.01	<0.01	<0.01	0.02	0.02	0.02	<0.01	<0.1	100.06	0.02	Q	0

3.2 Comminution Energy and GHG Emissions.

In this study, we fit a piecewise function to data on the energy required to achieve a target P80. This required employing a step-shape function from 1000 mm through 5 mm, the Bond Work Law equation between 5 mm and 0.03 mm, and a power function between 0.03 and 0.002 mm. Comminution

technologies consume large amounts of electricity when grinding to ultrafine particle sizes (< 0.01 to 0.02 mm) (**Figure 2**). Estimated energy to go from quarry to a final particle size of 0.179 mm is 23 kWh/t material. This is the same estimate as that reported by Huijgen and Comans.³⁴ Energy requirements to reduce quarry materials down to P80 5 mm vary from ~ 12 to 20 kWh/t in literature. Estimates more than double by just P80 of 0.06 mm, and increase exponentially beyond P80 0.01 mm. Our approach yields lower energy intensities for ultrafine particles than that predicted by Strefler and colleagues (**Figure 2**), reflecting the observed difference between their empirical model and values published and used in this study.⁷ Energy consumption at P80 less than 0.01 mm is lower in this analysis and in Shi and colleagues than that extrapolated by Strefler and colleagues⁷ due to the latter's use of a power function that underestimates SSA and subsequently overestimates comminution energy at grain size less than 0.01 mm.

At particle sizes < 0.01 mm, electricity source plays a critical role in CO_2 reductions, as carbon emissions can exceed 200 kg $\text{CO}_2\text{e/t}$ rock for equipment run on either the US or Pacific Gas and Electric (PG&E) electricity grid (**Figure 2**). Employing stir mills and emerging efficient comminution technologies can shield the EW process from being dependent on the availability of renewables for lowering emissions.³⁵ For example, the IsaMill and high pressure grinding rolls can reduce energy consumption by as much as 20% from ball mills.^{27,36} In this study, emissions from comminution appear minor in **Figure 2**, but represent the second largest source (**Table 2**).

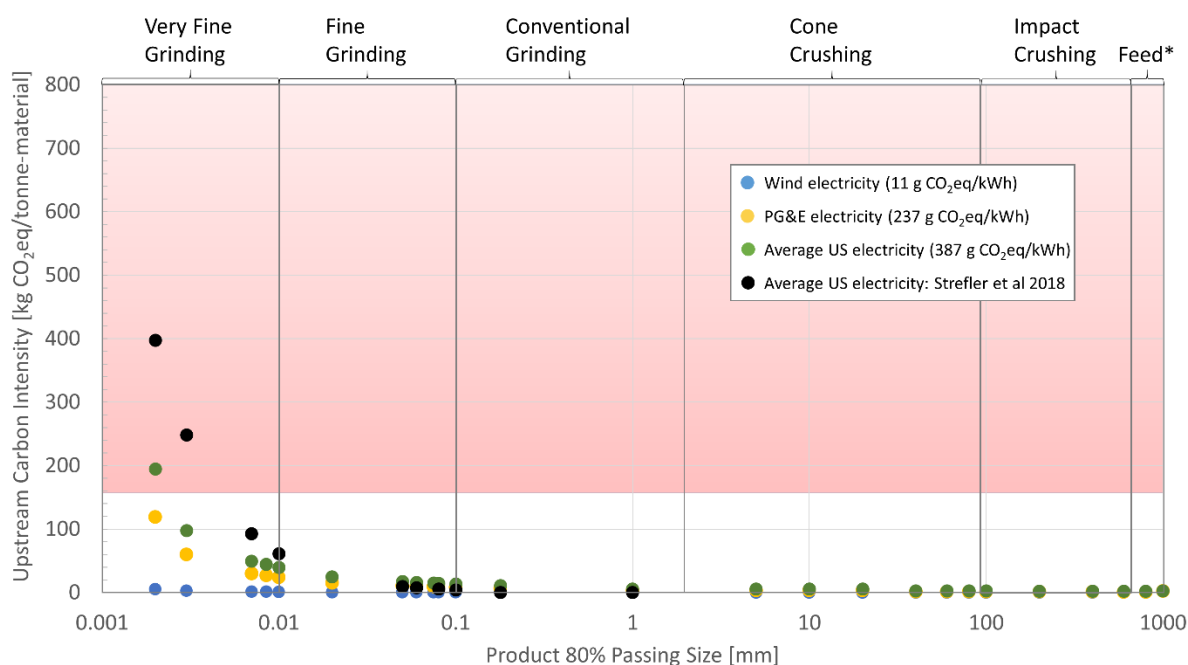


Figure 2. Upstream comminution carbon intensity based on an 80% product passing size and source of electricity. *Quarry blasting: assumed the emissions of limestone mining in UCLCI. Red indicates region where no life-cycle carbon removal is possible based on the E_{pot} of meta-andesite. The GHG emission intensities of electricity are listed in the legend. Pacific Gas & Electric: PG&E. United States: US.

3.3 Life-Cycle Impact Assessment

When accounting for all upstream emissions, we find that the effective net CDR of land-based EW using the olivine-bearing fines from Oregon can be as high as 658 kg CO₂e/t rock. The produced-for-purpose forsterite and olivine-bearing rock benchmarks achieve a net CDR of 898 and 723 kg CO₂e/t rock, respectively. Meanwhile, dacite and andesite fines from California offer more realistic net CDR of 101 and 136 kg CO₂e/t rock, respectively. At project scale, Oregon-sourced olivine-bearing fines achieve approximately 52,000 to 65,800 net t CO₂e sequestration. If a local source of olivine-bearing rock was established, even with comminution, net sequestration could increase to 72,200 net t CO₂e.

Approximately 15 years would be required to completely weather each of the 6 field applications of fines, suggesting a timeframe of 90 years for a project with a 1 mm material limit. For a project achieving 198 net t CO₂e/ha, this allows for the equivalent of 2.2 net t CO₂e/ha-year removal rate. Our measured SSA and dissolution during field trials with the meta-andesite sample suggest potentially more promising dissolution rates without further size reduction to 0.05 mm. Dissolution rates are uncertain, and experimental work conducted by some of the authors suggests an annual dissolution rate of 20%,³³ which would allow for nearly complete dissolution over a 30 year project. At the same time, reactive surface areas may decrease as carbonate minerals precipitate.

For materials with high E_{pot} , upstream process emissions are relatively small (4-5%) compared with the potential carbon removed (**Table 2**). Similar to other studies, transportation is a significant source of GHG emissions, at 43% of emissions for produced-for-purpose olivine-bearing rock in California, and 94% for olivine-bearing fines transported from Northern Oregon. In comparison, Taylor and colleagues⁹ estimate transportation to account for 88 to 96% of life cycle emissions of wollastonite application in a forested watershed. Quarry activities account for 48% of GHG emissions for produced-for-purpose small particle forsterite but only 1.5% of emissions for fines. We find that reducing diesel consumption would be more effective for lowering GHG emissions than switching to renewable electricity for the particle size range evaluated (0.05 to 0.179 mm). Loading and spreading on fields is nontrivial at 6 passes over 900 hectares, and accounts for 8% of emissions for the produced-for-purpose olivine-bearing rock in California (**Figure 4**).

Emissions from truck transport, loaders, electricity generation and transmission and field application can result in a large number of life cycle impacts (**Table S3**). Trucks transporting fines from Southern Oregon produce not only greenhouse gas emissions, but 20.2 t SO₂e which causes acidification, 411 t O₃e which leads to photochemical oxidant formation, and emissions such as particulate matter (4.2 t PM_{2.5}) which result in human health impacts in communities near transportation routes (163 disability-adjusted life years (DALY), which indicates the overall burden of disease based on ReCiPe 2016 endpoint (E)). These impacts should be considered alongside other technologies for carbon removal when weighing costs and benefits of each technology. If rocks are produced-for-purpose locally, electricity will result in higher emissions than transportation, particularly for impact categories such as eutrophication and particulate matter (**Figure 3A**).



Figure 3. Impact assessment results for EW on land in California. A) Scenario where produced-for-purpose rock material (0.179 mm) is transported from Ione, CA to Davis, CA. B) Scenario where quarry fines are transported from South Oregon to Davis, CA. DALY: disability-adjusted life years is an indicator of human health damages; PM_{2.5} is an indicator of human health damages; SO₂-e is an indicator of acidification; N-e is an indicator of eutrophication; CO₂-e is an indicator of Global Warming Potential.

3.4 Life-Cycle Cost

The cost of applying locally sourced fines is dominated by fines purchase price, collection and loading, and transportation, while the cost of using fines sourced from Oregon is mainly comprised of fines purchase price and transportation (**Figure 3A**). As expected, the produced-for-purpose local forsterite and olivine benchmark cases achieve a low levelized cost of net removal, at \$34 and \$43/net t CO₂e, respectively, with further size reduction down to 0.05 mm adding \$2/t-CO₂e. Of the real-world quarry byproduct rock samples evaluated, only the olivine-bearing fines from Southern Oregon achieve a cost lower than \$100, at \$96/net t CO₂e. Doubling the payload of trucks would reduce this value by \$43/net t CO₂e, while it would only lower the levelized cost of using produced-for-purpose forsterite or olivine-

bearing rock locally by \$5/net t CO₂e. Achieving a cost lower than \$100 for fines delivered from Southern Oregon depends of identifying fines with E_{pot} greater than 740 kg-CO₂/t rock, while it is unlikely materials from Northern Oregon will break \$100 (requiring of 1600 kg CO₂/t rock or higher). Alternatively, applying local fines from Ione, CA allows for E_{pot} as low as 260 kg CO₂/t rock.

The cost effectiveness of the technology is sensitive to the capacity factor, or annual production rate of material, and allowable application of material. For example, a company that invests in a given size equipment and truck fleet for 900 hectares who can now only apply olivine-bearing rock to 40 hectares would face an increased levelized cost dramatically up to \$228/net t CO₂e. Meanwhile, increasing allowable application rates to 111 t-material/ha would reduce cost to only \$38/net t CO₂e. The effects of decreasing area versus application rate while holding capital constant are somewhat different, despite both variables being used to determine the total amount of rock deployed in a project. This is due to explicit estimation of the number of tractors required per acreage, and the number of passes required to apply a given amount of rock at a thickness of 1 mm per hectare.

Other studies have placed a major emphasis on the impact of comminution electricity consumption and the potential for emissions and costs associated with grid electricity. We find that the use of grid versus renewable electricity had relatively small impact on GHG emissions and cost due to local grid characteristics even for scenarios with ball milling. Given the high consumption of diesel during the life cycle, operating in a location with cheap diesel or a cheap diesel substitute would be a more practical starting point for lowering costs, but would not lower emissions. Notably, andesite fines could achieve a cost lower than \$100 only with roundtrip transport distances below 40 km or diesel prices below \$0.83/L (\$3.15/gal), while dacite fines achieve a cost lower than \$100 at ultra-low diesel prices of \$1.28/L (\$2.43/gal). Under today's market conditions, we estimate the use of Northern California fines to cost \$174/t CO₂e or more, and Northern Oregon olivine-bearing fines to cost closer to \$260/t-CO₂e. Increasing E_{pot} by 70% for forsterite is at the upper bound of potentials estimated for silicate materials, and would lower levelized cost to ~\$21/t CO₂e which aligns with the lowest costs reported in literature. We conclude that such low costs do not represent realistic deployments of readily available quarry fines or produced-for-purpose rock.

Labor accounts for 15% of total costs and appears to be underestimated in previous analysis for large EW projects. A project of this size is expected to generate 5 to 12 full time jobs: 2 field workers, 1 to 8 drivers; and 1 to 2 quarry jobs. More jobs would be produced in regions with different requirements for shift hours, and jobs related to administration are also expected.

Table 2. Life-cycle GHG and cost results for select mineral samples for a 100,000 tonne-rock application project. Low and high values for the levelized cost of CDR include variations in transportation distance, particle size, the price of diesel and electricity, the emissions from electricity, bulk density, and tractor fuel efficiency. Low and high values do not include the impacts of SSA and E_{pot} which have to substantially higher impacts on cost and CDR and are discussed separately.

Sample	Supply Chain	Carbon Penalty kg CO ₂ eq/ t-rock	Levelized Cost (\$/tonne CO ₂ eq-net)			Project Removal t-CO ₂ eq	Life-Cycle Penalty %
			Low	High			
Forsterite 0.05 mm	Produced Ione California		36	20	97	89,800	4.2%
Forsterite 0.179 mm	Produced Ione California		34	18	97	90,000	3.9%
Olivine-bearing rock	Produced Ione California		43	23	108	72,200	4.9%
Olivine-bearing fines	Collected South Oregon		97	70	275	65,800	13.4%
Olivine-bearing fines	Collected North Oregon		260	112	350	52,100	31.4%
Meta-andesite fines	Collected Ione California		174	67	705	13,500	15.1%
Meta-dacite fines	Collected Ione California		235	90	1,200	10,000	19.3%
Olivine rock	Quarry Blasting	8.83					
Produced California	Quarry Transport	2.64					
	Comminution	6.91					
	Loading	0.60					
	Transport	17.00					
	Loading	0.60					
	Spread & Till	3.25					

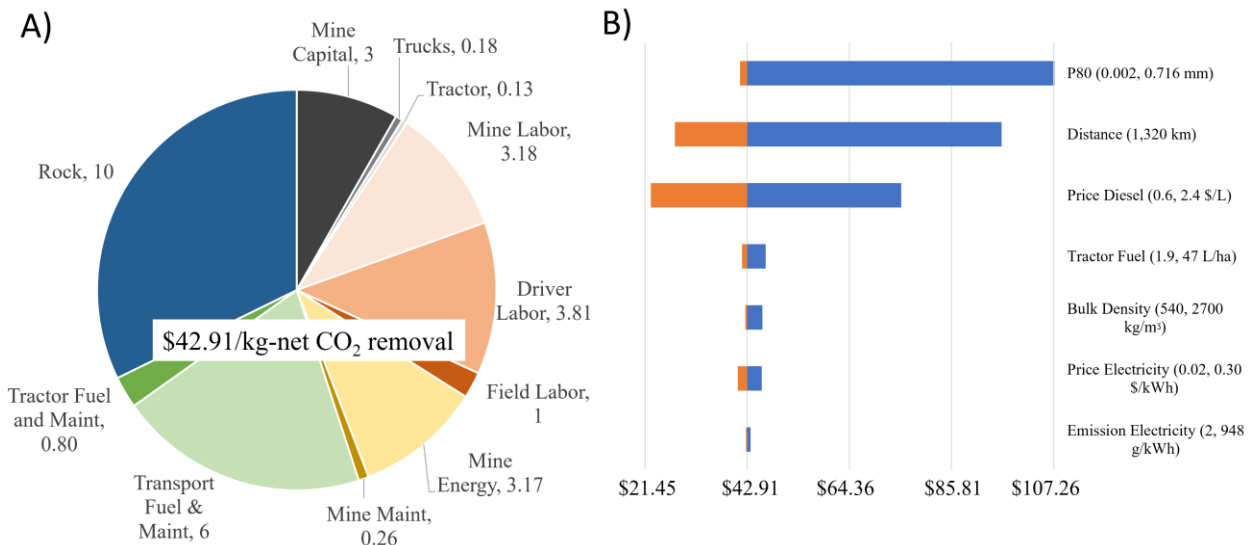


Figure 4. Breakdown of levelized installed capital and operating expenses for produced-for-purpose olivine rock at 0.179 mm. A) Pie chart of costs (\$/net t CO₂e removal) grouped by association with the capital, operation, and labor. B) Ranges in key market parameters reflect realistic lower and upper bound values gathered from market data and literature and resulting percent change on base case levelized cost.

3.5 Sensitivity and uncertainty of results

As noted in the previous section, there are several parameters characterizing the regional supply chain that can significantly influence cost, specifically: the requirement for ultra-small particles (P80), transport distance, diesel price and emissions, truck payload, tractor speed and fuel economy, driver and worker wages, bulk density and allowable application rate per project period (**Figure 4B**). All but the latter two are well defined. Wages will vary among truck fleets operators, farmers, and quarriers, while application rates may affect the duration materials are stored or collected from quarries. This plays an important role in the estimation of truck and tractor capital equipment. As seen in **Figure 4B**, System parameters that will be defined by project operators and location, specifically P80, distance, and the price of diesel, can increase costs by over 50%. Target grain size P80 affects particle SSA, and therefore dissolution rate, as well as comminution technology selection, cost and energy consumption. Without a limit on application rates, a smaller P80 improves the efficacy of EW for near-term carbon removal, but only increases costs.

Material loss, bulk density, and upfront capital costs for individual pieces of equipment represent more uncertain parameters in the analysis, and could potentially have a greater impact on levelized cost than what is estimated herein. Capital costs for representative equipment are gathered from vendors, but explicit power and energy consumption rates, as well as equipment lifespans were estimated using energy efficiency extrapolations and engineering rules of thumb. Further validation is needed regarding: the potential for siting new specialized equipment such as ball mills on quarries, the existence and operation patterns of quarry equipment that could be leveraged part of full time, and the starting price for small diameter materials such as fines that may be either stored at quarries or sold. Bulk density did not have a significant effect on base cost, but did influence the number of passes required for land application where there are thickness limits, and thus the necessary number of tractors, fuel consumption, and field labor hours. There is little reported data on bulk density for silicate materials at the grain sizes considered. Our review of densities of common powdered materials suggests particle density may be far lower than particle density at small mean particles sizes. However, at 0.179 mm, and based on reported data for basalt aggregate, we found 1800 kg/m³ to be a conservative estimate.

The approach presented in this analysis has limitations that make it difficult to determine if dissolution-correlated rates of CO₂ removal are optimistic or conservative. The range in SSA explored in this study do not result in 100% dissolution for forsterite or olivine over 30 years when a 1 mm application thickness is mandated. As noted previously, the olivine rock requires 90 years for application, however without the 1 mm limit, application would only take 15 years. When dividing project removal by hectares and 30 years, we find an average removal of 2.7 net t CO₂e per hectare per year for the olivine rock (0.89 at 90 years and 5.4 at 15 years). Even a single pass of forsterite would not dissolve in 30 years if SSA is 90% lower than our base value. It only takes ~50% reduction in SSA for the olivine sample at 0.179 mm to no longer achieve 100% dissolution of a single application of rock over the 30 year project. Similarly, the range in molar mass evaluated in Table S2 changed total dissolution from 17 to 2 years. Even without a limit on application thickness, it is sensible to divide applications into multiple years to reduce the necessary fines purchase and truck fleet in a single year.

Another limitation of this study is that the LCA approach does not capture production of particulate matter emissions from the rock material itself. We note that at a P80 of 0.179 mm, the particle distribution will include ultrafine material that may present a health hazard (particulate matter of 2.5 or 10 µm) or that

could potentially blow away during land application or truck transport. These impacts were not included in this analysis due to limited data. Discussions with several recent startup companies in land-based enhanced weathering suggest there is significant institutional knowledge between mines and agriculture for handling dusty materials and for minimizing unnecessary exposures and material loss that could allow for much greater application rates than 1 mm depth.

Finally, soil response and enhance biomass production are possible and should be explored as means of increasing overall life-cycle carbon removal. There is evidence that the application of EW rocks increases plant growth,^{8,9} but some minerals (e.g., olivine) introduce the potential for metals such as chromium and nickel to accumulate in agricultural soils^{37,38} and may necessitate limiting application to avoid imbalances in plant nutrition. Samples with high olivine concentrations can contain trace amounts of heavy metals such as Ni and Cr, and might warrant explicit routine soil tests and mineral tests.³⁹ Assuming material tests and labor intensive field tests add one cent to every tonne of material produced and increase field labor rates to \$200/hr, it is possible that the cost of local olivine-bearing rock EW could increase by 18%. The likelihood of contamination of olivine-bearing rocks is a key reason why identifying cost competitive EW using dacite and andesite fines bears great importance to the field.

3.6 Outlook

Production of aggregate is the second largest non-energy material produced in the United States, with growth expected as demand for construction materials rises. California is one of the largest producer of aggregate materials from pit and quarry operations, with numerous stone, sand, and gravel producers in California and Oregon overlay regions identified as promising for olivine-bearing rock and other rocks of interest for EW.^{21,40} At 51,000 thousand tonnes product and assuming 20 wt-% fines byproduct, California could produce as much as 10 million tonnes of fines from this industry. Quarry fines and mine tailings present an opportunity for EW due to the decreased need for new quarry activities and comminution which can have significant GHG emissions and environmental impacts.^{23,41,42} Assuming the tailings are purchased for \$10/t rock with no other mine associated costs, we find that tailings would require an E_{pot} of 260 kgCO₂/t rock or higher to achieve a levelized cost below \$100/net t CO₂e (or 160 kg CO₂/t rock, the same as andesite samples, if the cost of tailings is zero). This target CDR potential has been an important gap in recent literature, as highlighted in a recent review by Feng and Hicks.⁴³ Discussions with several startup companies in the EW space suggest the purchase of mine tailings and fines, as well as a focus on quarries instead of critical material mines is a promising pathway economically.

4. CONCLUSIONS

This study represents the first comprehensive analysis of the life-cycle greenhouse gas emissions and cost profile of land-based enhanced weathering at the scale of 100,000 tonne rock application (~3,000 net t CO₂e/yr sequestration) using rock samples representative of regional quarry materials. We develop and apply bottom-up models of key life-cycle phases representing real-world market and environmental conditions to estimate ranges in costs and emission rates. We find life cycle net CDR between 101-136 kg CO₂e/t rock for quarry fines evaluated without high olivine concentrations. Olivine-bearing rock fines

produced at quarries in Southern Oregon today can achieve a levelized cost of net carbon removal below \$100/net t CO₂e despite transportation distances to target agricultural lands in Northern California. The supply chains modeled achieved low costs at reasonable application rates (>25 t/ha), however costs and life cycle impacts would be substantially lower if a similar olivine-bearing quarry byproduct were to be identified locally. Rock samples representative of local fines, classified as meta-andesite and meta-dacite, did not perform as well, highlighting the importance of starting with high quality rock materials which may be scarce. At the same time, the samples evaluated appear to be more competitive than commercial direct air capture technologies, which have high costs of \$500 to 1000/t-CO₂ captured.⁴⁴ Even short transportation distances can still generate concerning local emissions from truck transport, and we highlight the importance of avoiding transportation through populated regions to reduce exposure to particulate matter and NO_x emissions.

Our results agree with recent estimates of cost for land-based EW achieving \$55 – 423/net t CO₂e. Like others, we find that annual hours of operation and transportation contribute significantly to emissions and cost. We note the importance of validating CDR and dissolution rates of recently acquired rock samples, as well as identify a gap in research related to the availability of fines and quarry byproducts. We identify several other supply chain uncertainties that require further validation: material loss and starting price, equipment type and performance at scale, truck fleet operation costs, and the impact of bulk density and application thickness allowances on annual material application.

As demonstrated in this study, expanding EW research to include materials beyond endmember minerals that would require dedicated quarries can provide insights on realistic geochemistry, and narrow down maximum allowable transportation and comminution costs. There is a limit, however, as it will be difficult for materials with E_{pot} between 160 and 260 kg CO₂/t rock to be cost competitive unless co-located with agriculture lands or provided completely free of charge. Through a diversity of scenarios evaluated, we have shown that starting with a promising material that requires some transportation is as economical as starting with a free weakly reactive material located right next to nearby land for treatment. Nevertheless, identifying ways to reduce the consumption of costly and emissive diesel in trucking is critical for developing EW as a sustainable and socially acceptable carbon removal technology.

DECLARATIONS OF INTEREST

PN is a member of the science advisory board and consultant for Terradot, Inc.

AUTHOR CONTRIBUTIONS

HMB: conceptualization, data curation, methodology, formal analysis, funding acquisition, visualization, writing original draft. PF: conceptualization, data curation, formal analysis. JD: writing original draft. RK, RJE, KZ: conceptualization, data curation. AV: conceptualization. HD, BA, PN: conceptualization, funding acquisition, project administration. All authors contributed to review and editing manuscript.

ACKNOWLEDGEMENTS

The authors gratefully acknowledge support from the U.S. Department of Energy under Contract No. DE-AC02-05CH11231 with the Lawrence Berkeley National Laboratory. The authors would like to

acknowledge the Laboratory Directed Research and Development (LDRD) Program at the Lawrence Berkeley National Laboratory for funding. The United States Government retains and the publisher, by accepting the article for publication, acknowledges that the United States Government retains a nonexclusive, paid-up, irrevocable, worldwide license to publish or reproduce the published form of this manuscript, or allow others to do so, for United States Government purposes. We thank the University of California Office of the President Working Lands Innovation Center (WLIC) for providing mineral samples and data. We thank an anonymous reviewer of this work for their generous guidance on rock classification.

REFERENCES

- (1) Schuiling, R. D.; Krijgsman, P. Enhanced Weathering: An Effective and Cheap Tool to Sequester CO₂. *Clim. Change* **2006**, *74* (1–3), 349–354. <https://doi.org/10.1007/S10584-005-3485-Y/METRICS>.
- (2) Köhler, P.; Hartmann, J.; Wolf-Gladrow, D. A. Geoengineering Potential of Artificially Enhanced Silicate Weathering of Olivine. *Proc. Natl. Acad. Sci. U. S. A.* **2010**, *107* (47), 20228–20233.
- (3) Hangx, S. J. T.; Spiers, C. J. Coastal Spreading of Olivine to Control Atmospheric CO₂ Concentrations: A Critical Analysis of Viability. *Int. J. Greenh. Gas Control* **2009**, *3* (6), 757–767. <https://doi.org/10.1016/j.ijggc.2009.07.001>.
- (4) Beerling, D. J.; Kantzas, E. P.; Lomas, M. R.; Wade, P.; Eufrazio, R. M.; Renforth, P.; Sarkar, B.; Andrews, M. G.; James, R. H.; Pearce, C. R.; Mercure, J. F.; Pollitt, H.; Holden, P. B.; Edwards, N. R.; Khanna, M.; Koh, L.; Quegan, S.; Pidgeon, N. F.; Janssens, I. A.; Hansen, J.; Banwart, S. A. Potential for Large-Scale CO₂ Removal via Enhanced Rock Weathering with Croplands. *Nat.* **2020**, *583* (7815), 242–248. <https://doi.org/10.1038/s41586-020-2448-9>.
- (5) Taylor, L. L.; Quirk, J.; Thorley, R. M. S.; Kharecha, P. A.; Hansen, J.; Ridgwell, A.; Lomas, M. R.; Banwart, S. A.; Beerling, D. J. Enhanced Weathering Strategies for Stabilizing Climate and Averting Ocean Acidification. *6* (4), 402–406. <https://doi.org/10.1038/nclimate2882>.
- (6) Fuss, S.; Lamb, W. F.; Callaghan, M. W.; Hilaire, J.; Creutzig, F.; Amann, T.; Beringer, T.; De Oliveira Garcia, W.; Hartmann, J.; Khanna, T.; Luderer, G.; Nemet, G. F.; Rogelj, J.; Smith, P.; Vicente, J. V.; Wilcox, J.; Del Mar Zamora Dominguez, M.; Minx, J. C. Negative Emissions - Part 2: Costs, Potentials and Side Effects. *Environ. Res. Lett.* **2018**, *13* (6), 063002. <https://doi.org/10.1088/1748-9326/AABF9F>.
- (7) Streffler, J.; Amann, T.; Bauer, N.; Kriegler, E.; Hartmann, J. Potential and Costs of Carbon Dioxide Removal by Enhanced Weathering of Rocks. *Environ. Res. Lett.* **2018**, *13* (3), 034010. <https://doi.org/10.1088/1748-9326/aaa9c4>.
- (8) ten Berge, H. F. M.; van der Meer, H. G.; Steenhuizen, J. W.; Goedhart, P. W.; Knops, P.; Verhagen, J. Olivine Weathering in Soil, and Its Effects on Growth and Nutrient Uptake in Ryegrass (*Lolium Perenne* L.): A Pot Experiment. *PLoS One* **2012**, *7* (8), 42098. <https://doi.org/10.1371/journal.pone.0042098>.
- (9) Taylor, L. L.; Driscoll, C. T.; Groffman, P. M.; Rau, G. H.; Blum, J. D.; Beerling, D. J. Increased Carbon Capture by a Silicate-Treated Forested Watershed Affected by Acid Deposition. *Biogeosciences* **2021**, *18* (1), 169–188.

- 654 (10) Sokol, N. W.; Sohng, J.; Moreland, K.; Slessarev, E.; Goertzen, H.; Schmidt, R.; Samaddar, S.;
655 Holzer, I.; Almaraz, M.; Geoghegan, E.; Houlton, B.; Montañez, I.; Pett-Ridge, J.; Scow, K.
656 Reduced Accrual of Mineral-Associated Organic Matter after Two Years of Enhanced Rock
657 Weathering in Cropland Soils, Though No Net Losses of Soil Organic Carbon. *Biogeochemistry*
658 **2024**, 167 (8), 989–1005. <https://doi.org/10.1007/S10533-024-01160-0/FIGURES/3>.
- 659 (11) Power, I. M.; Paulo, C.; Rausis, K. The Mining Industry's Role in Enhanced Weathering and
660 Mineralization for CO₂ Removal. *Environmental Science and Technology*. 2024, pp 43–53.
661 <https://doi.org/10.1021/acs.est.3c05081>.
- 662 (12) Holzer, I. O.; Nocco, M. A.; Houlton, B. Z. Direct Evidence for Atmospheric Carbon Dioxide
663 Removal via Enhanced Weathering in Cropland Soil. *Environ. Res. Commun.* **2023**, 5 (10),
664 101004. <https://doi.org/10.1088/2515-7620/ACFD89>.
- 665 (13) Deng, H.; Sonnenthal, E.; Arora, B.; Breunig, H.; Brodie, E.; Kleber, M.; Spycher, N.; Nico, P.
666 The Environmental Controls on Efficiency of Enhanced Rock Weathering in Soils. **2023**, 13 (1),
667 1–10. <https://doi.org/10.1038/s41598-023-36113-4>.
- 668 (14) Lefebvre, D.; Goglio, P.; Williams, A.; Manning, D. A. C.; de Azevedo, A. C.; Bergmann, M.;
669 Meersmans, J.; Smith, P. Assessing the Potential of Soil Carbonation and Enhanced Weathering
670 through Life Cycle Assessment: A Case Study for Sao Paulo State, Brazil. *J. Clean. Prod.* **2019**,
671 233, 468–481. <https://doi.org/10.1016/J.JCLEPRO.2019.06.099>.
- 672 (15) Foteinis, S.; Campbell, J. S.; Renforth, P. Life Cycle Assessment of Coastal Enhanced Weathering
673 for Carbon Dioxide Removal from Air. *Environ. Sci. Technol.* **2023**, 57 (15), 6169–6178.
- 674 (16) Feng, D.; Hicks, A. Environmental, Human Health, and CO₂ Payback Estimation and Comparison
675 of Enhanced Weathering for Carbon Capture Using Wollastonite. *J. Clean. Prod.* **2023**, 414,
676 137625. <https://doi.org/10.1016/J.JCLEPRO.2023.137625>.
- 677 (17) Zhang, B.; Kroeger, J.; Planavsky, N.; Yao, Y. Techno-Economic and Life Cycle Assessment of
678 Enhanced Rock Weathering: A Case Study from the Midwestern United States. *Environ. Sci.*
679 *Technol.* **2023**, 57 (37), 13828–13837.
- 680 (18) McQueen, N.; Kelemen, P.; Dipple, G.; Renforth, P.; Wilcox, J. Ambient Weathering of
681 Magnesium Oxide for CO₂ Removal from Air. *Nat. Commun.* 2020 111 **2020**, 11 (1), 1–10.
682 <https://doi.org/10.1038/s41467-020-16510-3>.
- 683 (19) Laboratory, N. R. E. *U.S. Life Cycle Inventory Database*.
684 <https://www.lcacommons.gov/nrel/search>.
- 685 (20) Renforth, P. The Potential of Enhanced Weathering in the UK. *Int. J. Greenh. Gas Control* **2012**,
686 10, 229–243.
- 687 (21) Krevor, S.; Graves, C.; Van Gosen, B.; McCafferty, A.; (US), G. S. Mapping the Mineral
688 Resource Base for Mineral Carbon-Dioxide Sequestration in the Conterminous United States.
689 *Usgs* **2009**.
- 690 (22) Renforth, P. The Negative Emission Potential of Alkaline Materials. **2019**, 10 (1), 1–8.
691 <https://doi.org/10.1038/s41467-019-09475-5>.

- 692 (23) Bullock, L. A.; James, R. H.; Matter, J.; Renforth, P.; Teagle, D. A. H. Global Carbon Dioxide
693 Removal Potential of Waste Materials From Metal and Diamond Mining. *Front. Clim.* **2021**, *3*,
694 694175. <https://doi.org/10.3389/FCLIM.2021.694175/BIBTEX>.
- 695 (24) Le Maitre, R. W. *Numerical Petrology. Statistical Interpretation of Geochemical Data*; 1982.
- 696 (25) Beerling, D. J.; Epihov, D. Z.; Kantola, I. B.; Masters, M. D.; Reershemius, T.; Planavsky, N. J.;
697 Reinhard, C. T.; Jordan, J. S.; Thorne, S. J.; Weber, J.; Martin, M. V.; Freckleton, R. P.; Hartley,
698 S. E.; James, R. H.; Pearce, C. R.; DeLucia, E. H.; Banwart, S. A. Enhanced Weathering in the US
699 Corn Belt Delivers Carbon Removal with Agronomic Benefits. *Proc. Natl. Acad. Sci. U. S. A.*
700 **2024**, *121* (9), e2319436121.
- 701 (26) Calabrese, S.; Wild, B.; Bertagni, M. B.; Bourg, I. C.; White, C.; Aburto, F.; Cipolla, G.; Noto, L.
702 V.; Porporato, A. Nano- to Global-Scale Uncertainties in Terrestrial Enhanced Weathering.
703 *Environ. Sci. Technol.* **2022**, *56* (22), 15261–15272. <https://doi.org/10.1021/ACS.EST.2C03163/>.
- 704 (27) Shi, F.; Morrison, R.; Cervellin, A.; Burns, F.; Musa, F. Comparison of Energy Efficiency
705 between Ball Mills and Stirred Mills in Coarse Grinding. *Miner. Eng.* **2009**, *22* (7–8), 673–680.
- 706 (28) Shi, F.; Lambert, S.; Daniel, M. A Study of the Effects of HPGR Treating Platinum Ores. In *SAG*
707 *2006*; 2006.
- 708 (29) Sandhu, G. S.; Christopher Frey, H.; Bartelt-Hunt, S.; Jones, E. In-Use Activity, Fuel Use, and
709 Emissions of Heavy-Duty Diesel Roll-off Refuse Trucks. **2015**, *65* (3), 306–323.
710 <https://doi.org/10.1080/10962247.2014.990587>.
- 711 (30) Hooper, A.; Murray, D. *An Analysis of the Operational Costs of Trucking : 2018 Update*; 2018.
- 712 (31) Parsons, S. D. *Estimating Fuel Requirements for Field Operations*; West Lafayette.
713 www.extension.purdue.edu/extmedia/AE/AE-110.html (accessed 2023-06-10).
- 714 (32) Energy/NETL, U. S. D. of. *Quality Guidelines For Energy System Studies; Cost Estimation*
715 *Methodology for NETL Assessments of Power Plant Performance, NETL-PUB-22580*; 2019.
- 716 (33) Kumar, R.; Arora, B.; Deng, H.; Sonnenthal, E. L.; Eloy Alves, R. J.; Breunig, H.; Fox, P. M.; Di
717 Vittorio, A. V.; Zhalnina, K.; Brodie, E.; Nico, P. S.; Kumar, R.; Arora, B.; Deng, H.; Sonnenthal,
718 E. L.; Eloy Alves, R. J.; Breunig, H.; Fox, P. M.; Di Vittorio, A. V.; Zhalnina, K.; Brodie, E.;
719 Nico, P. S. Influence of Precipitation and Temperature Variations on Enhanced Rock Weathering
720 for Negative Carbon Emissions: A Modeling Perspective. *AGUFM* **2022**, *2022*, SY45B-0647.
- 721 (34) Huijgen, W. J. J.; Comans, R. N. J. Carbonation of Steel Slag for CO₂ Sequestration: Leaching of
722 Products and Reaction Mechanisms. *Environ. Sci. Technol.* **2006**, *40* (8), 2790–2796.
723 <https://doi.org/10.1021/es052534b>.
- 724 (35) Curry, J. A.; Ismay, M. J. L.; Jameson, G. J. *Mine Operating Costs and the Potential Impacts of*
725 *Energy and Grinding*; Pergamon, 2014; Vol. 56, pp 70–80.
- 726 (36) Gurnett, I.; Waal, H. De; Stieper, G. The IsaMillTM - 25 Years of Stirred Milling.
- 727 (37) Beerling, D. J.; Leake, J. R.; Long, S. P.; Scholes, J. D.; Ton, J.; Nelson, P. N.; Bird, M.; Kantzas,
728 E.; Taylor, L. L.; Sarkar, B.; Kelland, M.; DeLucia, E.; Kantola, I.; Müller, C.; Rau, G.; Hansen, J.

729 Farming with Crops and Rocks to Address Global Climate, Food and Soil Security. **2018**, *4* (3),
730 138–147. <https://doi.org/10.1038/s41477-018-0108-y>.

731 (38) Renforth, P.; Pogge von Strandmann, P. A. E.; Henderson, G. M. The Dissolution of Olivine
732 Added to Soil: Implications for Enhanced Weathering. *Appl. Geochemistry* **2015**, *61*, 109–118.

733 (39) Haque, F.; Chiang, Y. W.; Santos, R. M. Risk Assessment of Ni, Cr, and Si Release from Alkaline
734 Minerals during Enhanced Weathering. *Open Agric.* **2020**, *5* (1). [https://doi.org/10.1515/opag-](https://doi.org/10.1515/opag-2020-0016)
735 2020-0016.

736 (40) McFaul, E. J.; Geological Survey (U.S.). U.S. Geological Survey Mineral Databases, MRDS and
737 MAS/MILS. *U S Geological Survey digital data series DDS-52*. 2000.

738 (41) Power, I. M.; Dipple, G. M.; Bradshaw, P. M. D.; Harrison, A. L. Prospects for CO₂
739 Mineralization and Enhanced Weathering of Ultramafic Mine Tailings from the Baptiste Nickel
740 Deposit in British Columbia, Canada. *Int. J. Greenh. Gas Control* **2020**, *94*, 102895.
741 <https://doi.org/10.1016/J.IJGGC.2019.102895>.

742 (42) Stokreef, S.; Sadri, F.; Stokreef, A.; Ghahreman, A. Mineral Carbonation of Ultramafic Tailings:
743 A Review of Reaction Mechanisms and Kinetics, Industry Case Studies, and Modelling. *Clean.*
744 *Eng. Technol.* **2022**, *8*, 100491. <https://doi.org/10.1016/J.CLET.2022.100491>.

745 (43) Feng, D.; Hicks, A. Environmental, Human Health, and CO₂ Payback Estimation and Comparison
746 of Enhanced Weathering for Carbon Capture Using Wollastonite. *J. Clean. Prod.* **2023**, *414*,
747 137625. <https://doi.org/10.1016/J.JCLEPRO.2023.137625>.

748 (44) *Negative Emissions Technologies and Reliable Sequestration*; National Academies Press, 2019.
749 <https://doi.org/10.17226/25259>.

750